11th International Workshop on Ship and Marine Hydrodynamics
Hamburg, Germany, September 22-25, 2019

Experimental and Numerical Study for Weathervane and Stability Performance of Single-Point-Moored FOWTs Under Wind-Current Coexisting Field

K. Hashimoto[1,*], S. Srinivasamurthy[1], K.Iijima[2] , Y. Nihei[1]

[1]Osaka Prefecture University, Department of Aerospace and Marine System Engineering
1-1 Gakuen-cho, Naka-ku, Sakai, Osaka 599-8531, Japan
[2]Osaka University, Department of Naval Architecture
1-1 Yamada, Suita, Osaka 565-0871, Japan

*Kazuki Hashimoto, syb03091@edu.osakafu-u.ac.jp

ABSTRACT

In this study, the weathervane and stability performance of Floating Offshore Wind Turbines (FOWTs) moored to Single-Point-Mooring (SPM) system in the wind and current coexisting field is considered through a series of experiments and numerically simulating time-series history. First, we designed and manufactured scaled models of two types FOWTs, a semi-submersible and spar, based on Froude's scaling law. The scaled models are experimented in a circulating water tank at Osaka Prefecture University, Osaka, Japan. It was found out that the weathervane performance of both the FOWTs types was acceptable in rated wind and slow speed current condition. However, in the rated wind and high speed current condition, the weathervane performance especially of the semi-submersible type was not acceptable and instability oscillation of spar type was observed. In addition, a numerical simulation program was developed assuming the SPM-FOWTs modelled as two rigid bodies. In this time history program, the effect of the bearing on the mooring buoy is considered for clear understanding. The result of the program is discussed and compared to the results of the experiments.

1 INTRODUCTION

Recently, FOWTs are attracting a great deal of attention as offshore renewable energy source in terms of its energy efficiency and potential. In Japan, various projects about the FOWTs are underway, including the Fukushima floating wind farm demonstration project [1], funded by the Ministry of Economy, Trade and Industry of Japan. Wind turbines normally weathervane using the yaw control system inside the nacelle. However, the yaw control system is found to be one of the major reasons for the failure of wind turbines [2]. A vane anemometer failure or power failure due to a storm or lightning make it impossible to control the yaw direction. And it may cause severe failures such as blade breakage and structural failure. Especially, in the case of Floating Offshore wind turbines, when the yaw control system breaks down, it becomes all the more difficult to repair it on the sea because of the high altitude and waves. Also, if the failure is severe, the wind turbine needs to be towed back to docks. And it increases maintenance costs because the costs of removing and setting up the moorings and towing FOWT are quite expensive. As one of the solutions of this problem, Single Point Mooring system is proposed by some of the present authors [3][4].

SPM system consists of a buoy with a rotation mechanism such as a bearing, and a connection. The FOWT is attached to the buoy moored to the seabed through the connection, which allows the FOWT to rotate around the buoy. By introducing SPM system to FOWTs, it becomes possible for FOWTs to follow the wind direction by using only wind force. As a result, since the yaw system becomes unnecessary and rotation mechanism acts at a lower position, the maintenance performance and the top-heaviness is improved. In addition, there is an advantage that the buoy and FOWT can be attached and detached easily when the FOWT needs to be towed back to docks. On the other hand, it poses technical challenges to put this system

into practical use in the real sea area. Especially, the ocean current greatly affects the stability and weathervane performance of FOWTs moored to SPM system. Therefore, it is important to understand the behaviour of the FOWTs moored to SPM system under the condition where wind and current are coexisting. In this paper, two types of FOWTs (Spar type and Semi-Submersible type) are considered, and its stability and weathervane performance in the wind-current coexisting field is compared in terms of the experiment and numerical simulation.

2 SCALED MODEL OF FOWTS

In this section, the detail of scaled models of FOWTs used in experiments are explained. The 5MW wind turbine are scaled down to 1/200 scale. The scaled models are designed and manufactured based on Froude scaling law.

2.1 Wind turbine model

The wind turbine model refers to the 5MW wind turbine designed by NREL [5]. Figure 1 shows the scaled model of the wind turbine. This model is made of urethane and FRP (Fibre Reinforced Plastic). Table 1 shows the principal particulars of the wind turbine model.

Figure 1: Wind turbine 1/200 scaled model

Table 1: Principal particulars of wind turbine model

Item	Value	Unit
Hub diameter	630	mm
Hub height	450	mm
Tower base diameter	30	mm
Tower top diameter	20	mm
Rotor + Nacelle mass	53.5	g
Tower mass	35.2	g
Wind turbine type	Downwind-type	
Airfoil	NACA4412	

2.2 Spar type model

Figure 2 shows the scaled model of spar type. The spar type scaled model is designed considering the stability and constructability, natural period for wave period, etc. This scaled model consists of combination of several acrylic columns. Spar type has a middle column and a ballast column. The middle column plays a role in raising the center of buoyancy and lowering the draft for application in intermediate water depth. The ballast column plays a role in lowering the center of gravity, improving the stability of the FOWT.

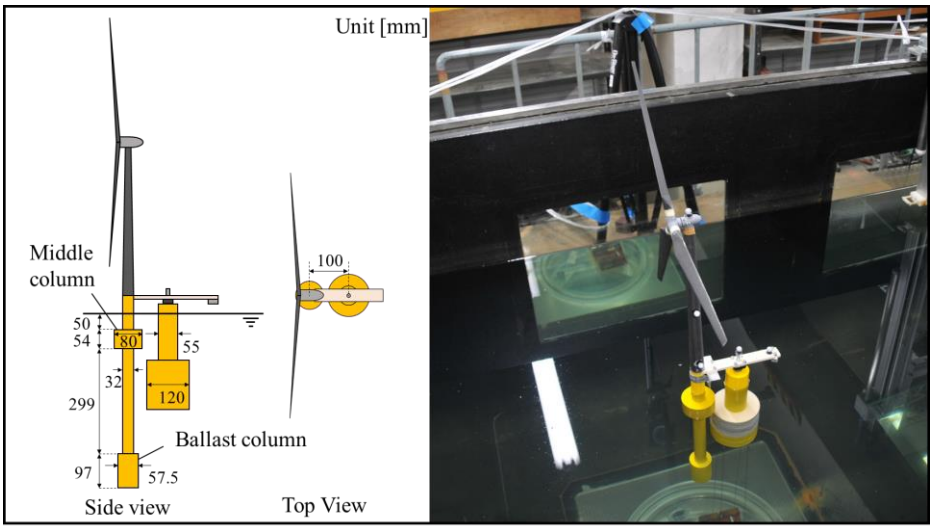

Figure 2: Spar type scaled model

Spar type floater is attached to the buoy with bearing on the top through the rigid bar. The buoy is moored by tension leg mooring. Therefore, the spar type floater can rotate around the buoy. The distance from spar type floater to buoy is 10.0 cm.

Table 2 shows the principal particular of spar type. Spar type scaled model weighs about 800 grams which corresponds to about 6400 tons in real scale. And the draft of scaled model corresponds to 100 m in real scale.

Table 2: Principal particulars of spar type scaled model

Item	Value	Unit
Displacement	804	g
Diameter of water plane	32.0	mm
Draft	500.0	mm
Position of middle column (upper area)	50.0	mm
Diameter / Length of middle column	80.0 / 54.0	mm
Position of ballast column (upper area)	403.0	mm
Diameter / Length of ballast column	57.5 / 97.0	mm
GM (with wind turbine)	36.9	mm

2.3 Semi-Submersible type model

Figure 3 shows the scaled model of Semi-Submersible type. This model is designed and manufactured based on the model proposed by Osaka University [6]. This scaled model consists of three columns and a lower hull. The columns play a role in improving the stability of this model and lower hull provides integrity in fixing these three columns and lowering the center of gravity.

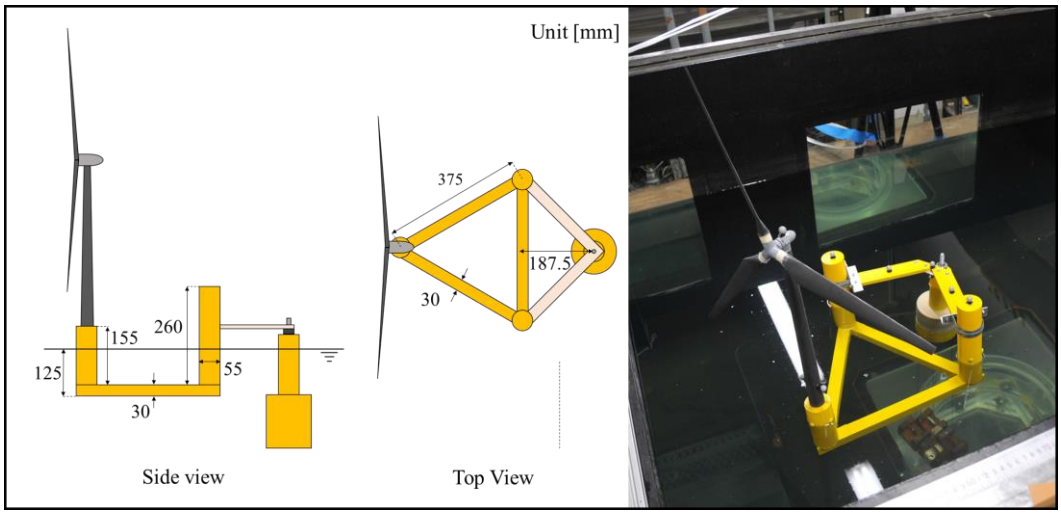

Figure 3: Semi-Submersible type scaled model

Two columns of Semi-submersible type are connected to the buoy with bearing on the top through a rigid yoke structure. The buoy is moored by tension leg mooring. Then, Semi-Submersible type floater can rotate around the buoy. The distance from the column housing the wind turbine to the buoy is 512.3 mm.

Table 3 shows the principal particular of Semi-Submersible type. Semi-Submersible type scaled model weighs about 1.7 kilograms which corresponds to about 13600 tons in real scale.

Table 3: Principal particulars of Semi-Submersible type scaled model

Item	Value	Unit
Displacement	1690.0	g
Draft	125.0	mm
Distance between columns	375.0	mm
Column diameter	55.0	mm
Column length (tower part)	260.0 (155.0)	mm
Lower hull breadth	30.0	mm
Lower hull depth	30.0	mm
GM	32.9	mm

3 CIRCULATING WATER TANK TEST

In this section, the outline of the water tank tests using the 1/200 scaled model in wind and current coexisting field are explained. A circulating water tank and a wind blower is set to generate current and wind. Figures 4 and 5 show the circulating water tank and wind blower used in the experiment. The length, breadth and depth of circulating water tank is respectively 4.5, 1.5 and 1.0 meters. The wind blower consists of six fans and a control panel.

Figure 4: Circulating water tank

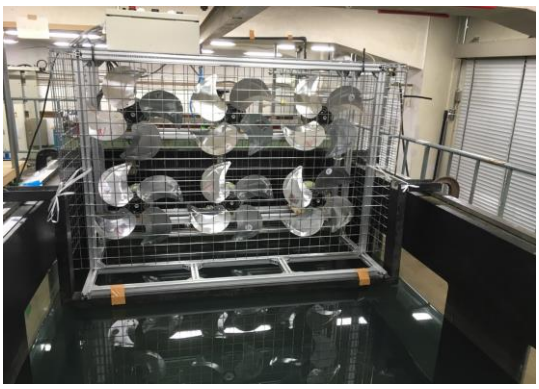

Figure 5: Wind blower

3.1 Experimental conditions

The experiment is conducted by changing the current speed and initial yaw angle. Wind and current are setup opposite to each other during experiment. Table 4 shows the conditions of the experiments.

Table 4: Experimental conditions

Item	Value	Unit
Types of floating body	Spar, Semi-Submersible	-
Wind speed	2.2 (Rated thrust)	m/s
Current speed	0, 3.69, 7.23, 11.0	cm/s
Initial angle of FOWTs	0, 45, 90, 135, 180, 225, 270, 315	degree

The wind speed is fixed at 2.2[m/s] and it corresponds to the rated thrust value in real scale based on the Froude scaling law. Current speeds of 3.69, 7.23 and 11.0 cm/s correspond to 1.0, 2.0 and 3.0 knots in real scale.

Figure 6 shows the initial yaw angle of FOWTs. After the scale model is placed at each initial yaw angle, wind and current are turned on. Then the stability and weathervane performance are observed. Yaw angle of 180° is the final point where the downwind-type FOWT stabilize following the wind.

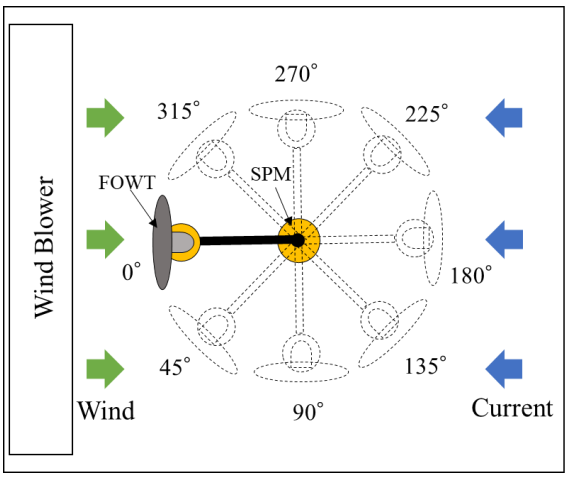

Figure 6: Initial yaw angle of FOWT

3.2 Measurement method

The measuring items used in the experiment are motion capture camera and tracker. Figure 7 shows the (a) motion capture camera and (b) tracker. By irradiating light and measuring the reflection light from tracker with two cameras, the 6-DoF data can be obtained. Therefore, it is possible to obtain time series data of motion.

(a) Motion capture camera (b) Tracker

Figure 7 Motion capture device

4 NUMERICAL SIMULATION

In this section, numerical simulation methodology is explained. The simulation considers the 3-DoF motions in the horizontal plane. The SPM-FOWT system is considered as a combination of two rigid bodies of a FOWT with a connecting bar and a mooring buoy. The two rigid bodies are assumed to be connected by a bearing with friction. Also, this simulation considers wind, current and mooring as external forces.

4.1 Equation of motion

The equation of motion is introduced as two rigid bodies, FOWT with a connecting bar and a mooring buoy. Figure 8 shows the coordinate systems of this model. The mooring buoy is expressed in an absolute coordinate system (a). FOWT is attached to the center of mooring buoy, and the yawing motion of the FOWT is considered (b).

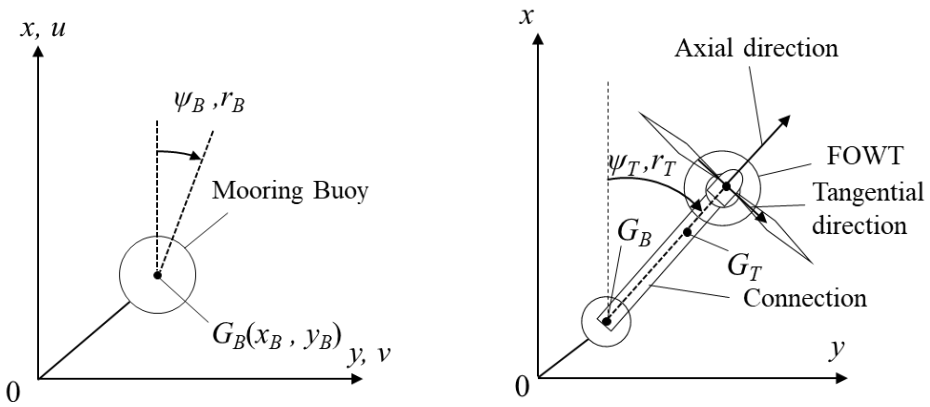

(a) Mooring buoy (b) FOWT with connecting bar

Figure 8: The coordinate system

In Figure 8, $\boldsymbol{G}_B(x_B, y_B)$ is the buoy center and ψ_B is the yaw angle of the mooring buoy. $\boldsymbol{G}_T$ and ψ_T are the location of the gravity point and yaw angle of FOWT with connecting bar. The mooring buoy motion of equation in surge, sway and yaw directions can be written as,

$$m_B \frac{d^2 x_B}{dt^2} = T_x + F_{BCx} + F_{TBr} \cos\psi_T + F_{TB\psi} \sin\psi_T \tag{1}$$

$$m_B \frac{d^2 y_B}{dt^2} = T_y + F_{BCy} + F_{TBr} \sin\psi_T - F_{TB\psi} \cos\psi_T \tag{2}$$

$$I_B \frac{d^2 \psi_B}{dt^2} = T_M + M_{TB} \tag{3}$$

Where, m_B and I_B are the mass and the moment of inertia of the mooring buoy. T_x, T_y and T_M are the force in the x and y directions and the yaw moment acting on the buoy due to mooring. F_{BCx} and F_{BCy} are the force in the x and y directions acting on the FOWT due to current. F_{TBr} and $F_{TB\psi}$ are respectively the axial and tangential internal force between the mooring buoy and the FOWT. M_{TB} is the moment caused by friction of the bearing on the buoy.

The equation of motion for the FOWT with the connecting bar in axial and tangential direction can be written as,

$$F_{TWr} + F_{TCr} - F_{TBr} - m_T \frac{d^2 x_B}{dt^2}\cos\psi_T + m_T \frac{d^2 y_B}{dt^2}\sin\psi_T = 0 \tag{4}$$

$$I_T \frac{d^2\psi_T}{dt^2} = F_{TW\psi}\cdot L_2 + F_{TC\psi}\cdot L_3 + M_Z - M_{TB} + m_T \frac{d^2 x_B}{dt^2} L_1 \sin\psi_T - m_T \frac{d^2 y_B}{dt^2} L_1 \cos\psi_T \tag{5}$$

Where, m_T and I_T are the mass and the moment of inertia of the FOWT. F_{TWr}, $F_{TW\psi}$ and M_Z are the axial and tangential force and yaw moment acting on the FOWT due to wind. F_{TCr} and $F_{TC\psi}$ are axial and tangential current force. L_1 is the distance between $\boldsymbol{G}_B$ and $\boldsymbol{G}_T$. L_2 is the distance between $\boldsymbol{G}_B$ and the point of action of wind force. L_3 is the distance between $\boldsymbol{G}_B$ and the point of action of current force.

4.2 Modeling of wind force

The wind load on the wind turbine varies by the angle of attack of the wind. In this study, the wind load measured by a dynamometer is applied to the simulation. The wind load F'_{TWr}, $F'_{TW\psi}$ [N] and M'_Z [N m] (Figure 9) at wind speed of 2.2[m/s] is measured by changing the inflow angle by 15 degrees. Figures 10 and 11 show the measured wind load. The point between measurement points is interpolated by spline.

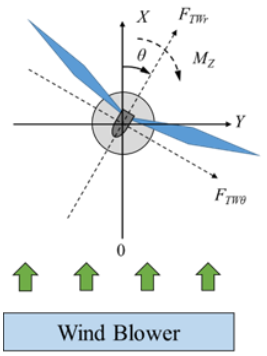

(a) Measurement Items (b) Image of measurement

Figure 9: Measurement of wind load

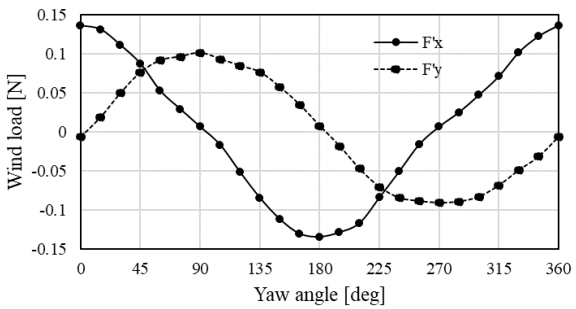

Figure 10: Wind load Fx, Fy in 1/200 scaled model

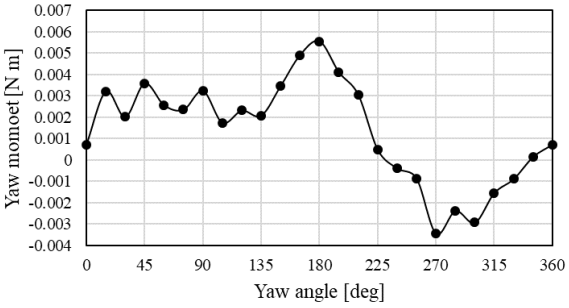

Figure 11: Wind load Mz in 1/200 scaled model

Measured wind load $\boldsymbol{F}'_W$ can be assumed as follow

$$\boldsymbol{F}'_W = \frac{1}{2}\boldsymbol{C}_{DW}\rho_A V'^2_W A_W \tag{6}$$

Where, $\boldsymbol{C}_{DW}$ is drag coefficient, ρ_A [kg/m^3] is air density, V_W' is wind speed of 2.2[m/s], A_W [m^2] is projected area of wind turbine. Assuming that $\boldsymbol{C}_W$, ρ_A and A_W are constant, wind load $\boldsymbol{F}_W$ at relative wind speed V_W is given as,

$$\boldsymbol{F}_W = \boldsymbol{F}_W' \, V_W^2 \Big/ V_W'^2 \tag{7}$$

The yaw moment M_Z on the wind turbine is also given as follows,

$$M_Z = M_Z' \, V_W^2 \Big/ V_W'^2 \tag{8}$$

The relative wind speed V_W and inflow relative angle θ_W considering the movement of buoy and FOWT is given as follows.

$$\boldsymbol{V}_W = \begin{pmatrix} V_{Wr} \\ V_{W\psi} \end{pmatrix} = \begin{pmatrix} -V_{W0}\cos(\psi_T - \varphi_W) - u\cos\psi_T - v\sin\psi_T \\ V_{W0}\sin(\psi_T - \varphi_W) + u\sin\psi_T - v\cos\psi_T - rL_2 \end{pmatrix} \tag{9}$$

$$\theta_W = \tan^{-1}\left(\frac{V_{W\psi}}{V_{Wr}}\right) \tag{10}$$

Where, V_{W0} is absolute wind speed. Therefore, wind force is given as,

$$F_{TWr} = F_W \sin\theta_W, \qquad F_{TW\psi} = F_W \cos\theta_W \tag{11}$$

4.3 Modeling of current force

In this study, current force is assumed as follows

$$F_C = \frac{1}{2} C_D \rho_W V_C^2 A_C \tag{12}$$

Where, $\boldsymbol{C}_D$ is drag coefficient, ρ_W [kg/m^3] is water density, V_C is relative current speed, A_C [m^2] is projected area under the water. The relative current speed V_C and inflow relative angle θ_C considering the movement of buoy and FOWT is given as follows.

$$\boldsymbol{V}_C = \begin{pmatrix} V_{Cr} \\ V_{C\psi} \end{pmatrix} = \begin{pmatrix} -V_{C0}\cos(\psi_T - \varphi_C) - u\cos\psi_T - v\sin\psi_T \\ V_{C0}\sin(\psi_T - \varphi_C) + u\sin\psi_T - v\cos\psi_T - rL_3 \end{pmatrix} \tag{13}$$

$$\theta_C = \tan^{-1}\left(\frac{V_{C\psi}}{V_{Cr}}\right) \tag{14}$$

$$F_{TCr} = F_C \sin\theta_C, \qquad F_{TC\psi} = F_C \cos\theta_C \tag{15}$$

4.4 Modeling of mooring force

In the experiment, the buoy is moored by four cables and anchor. The mooring force acted by i-th mooring T_i [N] is assumed as,

$$T_i = k \cdot \delta \tag{16}$$

Where, k [N/m] is the mooring coefficient, and δ is Displacement of i-th mooring point of the buoy. When the i-th mooring point moves from initial mooring position (x_i, y_i) to the position (x_i', y_i'), (x_i, y_i) is given as,

$$\begin{pmatrix} x_i' \\ y_i' \end{pmatrix} = \begin{pmatrix} \cos\psi_B & -\sin\psi_B \\ \sin\psi_B & \cos\psi_B \end{pmatrix} \begin{pmatrix} x_i \\ y_i \end{pmatrix} + \begin{pmatrix} x_B \\ y_B \end{pmatrix} \tag{17}$$

Therefore, the angle α_i , the mooring force T_{xi} and T_{yi}, the moment T_{Mi} is given as follows.

$$\alpha_i = \tan^{-1}\left(\frac{y_i' - y_i}{x_i' - x_i} \right) \tag{18}$$

$$T_{xi} = -T_i \cos\alpha_i \,,\; T_{yi} = -T_i \sin\alpha_i \tag{19}$$

$$T_{Mi} = -T_i L_i \sin(\alpha_i - \psi_B) \tag{20}$$

Where, L_i is the distance between center of buoy and i-th mooring point. T_x , T_y and T_M can be calculated as the sum of the four moorings.

$$T_{x,y} = \sum_{i=1}^{4} T_{xi,yi} \;,\; T_M = \sum_{i=1}^{4} T_{Mi} \tag{21}$$

4.5 Modeling of bearing

In the experiment, a bearing is used as the rotation mechanism between the mooring buoy and FOWT with connecting bar. When the tangential internal force $F_{TB\psi}$ acts, the friction moment of the bearing M_{TB} is generated.

$$M_{TB} = \mu P \frac{d}{2} \tag{22}$$

Where, μ [-] is the coefficient of friction, d [m] is the nominal bearing inner diameter. P is the resultant load acting on the bearing estimated as,

$$P = \sqrt{F_{TBr}^2 + F_{TB\psi}^2} \tag{23}$$

When the axial internal force F_{TBr} acts on the FOWT, the axial force of the same magnitude is generated as an internal force on the buoy. When the yaw moment of the wind turbine M_Z act, the tangential force $F_{TB\psi}$ is generated as an internal force.

$$F_{TB\psi} = \frac{Mz}{L_2} \tag{24}$$

4.6 Conditions of the simulation

Table 5 shows the condition of the simulation. Runge-Kutta-Gill method is adopted in the simulation as the time history calculation method. And the time step is 0.05 [sec].

Table 5: Conditions of the simulation

Items	Value		Unit
	Spar	Semi-Submersible	
m_B	0.347	0.347	kg
I_B	5.53×10^{-3}	5.53×10^{-3}	Kg m^2
m_T	0.904	1.790	kg
I_T	8.36×10^{-3}	2.08×10^{-1}	Kg m^2
L_1	0.050	0.316	m
L_2	0.115	0.512	m
L_3	0.100	0.296	m

5 EXPERIMENTAL AND SIMULATION RESULT

5.1 Only wind condition

Figures 12 and 13 show the experimental and simulation result of spar type and Semi-Submersible type in the only wind conditions. The FOWT start rotating around the mooring buoy at initial angle of 0 degree, and aligns itself with the wind direction to final position at around 180 degrees.

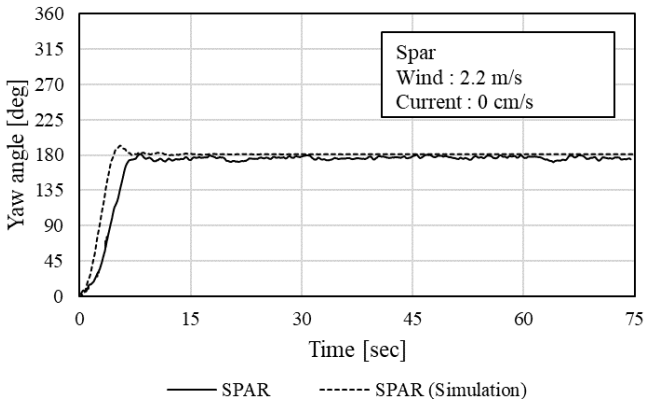

Figure 12: Only wind condition of spar type.

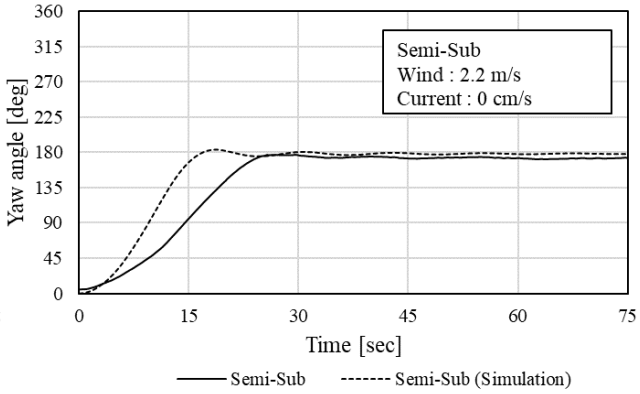

Figure 13: Only wind condition of Semi-Submersible

Both of the models can follow the wind direction finely. And it can be said that the models attain stability. Comparing the results of spar and Semi-Submersible, spar type follows the wind faster than Semi-Submersible type. The main reason for such a difference of response speed is due to the yaw moment caused by current load. The response speed may be closely related to power generation rate. Thus, a FOWT with early response to wind direction is advantageous for weathervane performance.

Comparing the experimental and simulation results, the simulation attains stability faster than the experiment in both the results of spar and semi-submersible. This can be because the damping force due to water is not considered in the simulation.

5.2 Wind-Current coexisting condition

In this section, wind-current coexisting condition is considered. Current speeds are varied from 3.69 cm/s to 11 cm/s. Figures 14 and 15 show the (a) experimental and (b) simulation results of spar type and Semi-Submersible type in the wind-current coexisting condition (V_{w0} = 2.2 cm/s, V_{c0} = 3.69 cm/s).

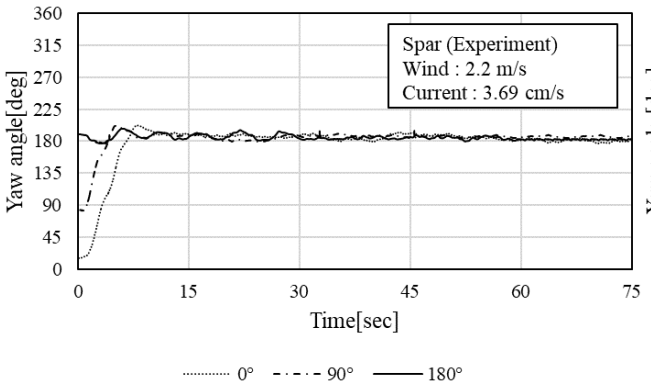

(a) Experimental result

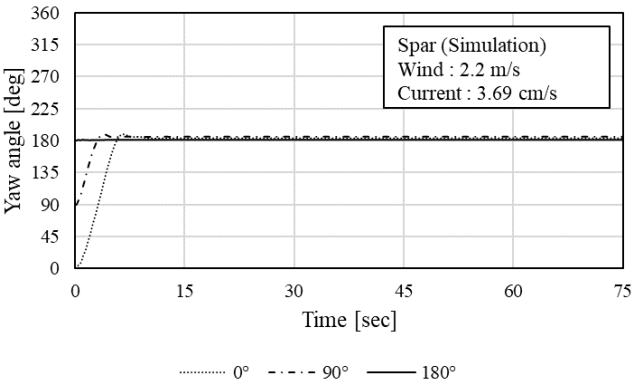

(b) Simulation result

Figure 14: Spar model in wind-current coexisting condition(V_{w0} = 2.2 cm/s, V_{c0} = 3.69 cm/s)

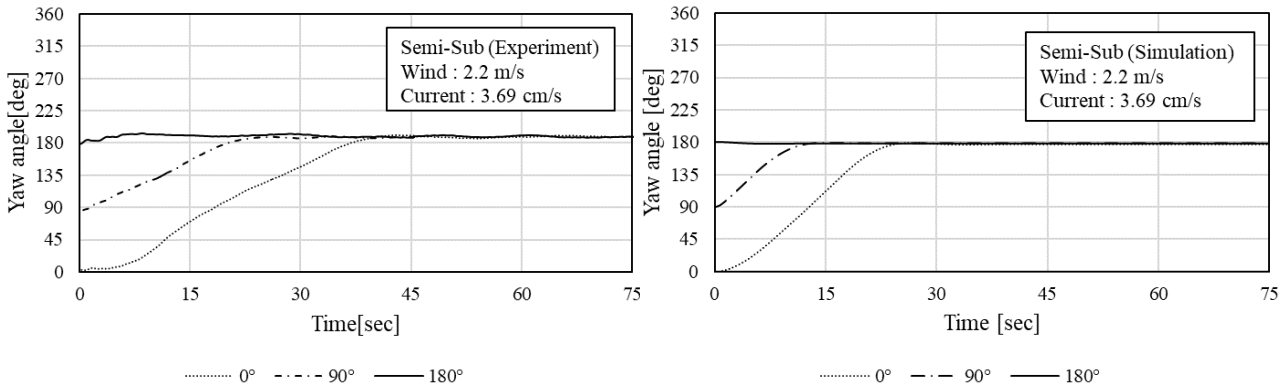

(a) Experimental result (b) Simulation result

Figure 15: Semi-Sub model in wind-current coexisting condition (V_{w0} = 2.2 cm/s, V_{c0} = 3.69 cm/s)

It can be observed that both of the models can follow the wind direction. A minute vibration can be observed for spar model. However, the vibration is so small that is can be said to be stable. Response time can be defined as the time taken for the FOWT to attain the final position from the initial position. Comparing the experimental results of spar and Semi-Submersible, spar type follows the wind direction much faster. The response time tends to increase, as the current speed increases. This is because the current force interferes with the wind force. Similar to the only wind condition, the simulations tend to follow the wind direction faster than the experiments.

Figures 16 and 17 show the (a) experimental and (b) simulation results of spar type and Semi-Submersible type in the wind-current coexisting condition (V_{w0} = 2.2 cm/s, V_{c0} = 7.23 cm/s).

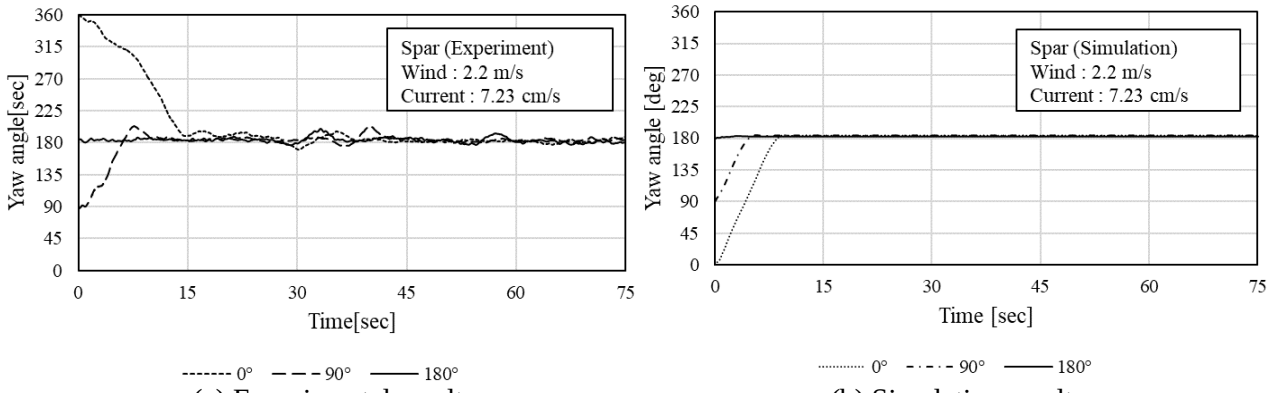

(a) Experimental result (b) Simulation result

Figure 16: Spar model in wind-current coexisting condition (V_{w0} = 2.2 cm/s, V_{c0} = 7.23 cm/s)

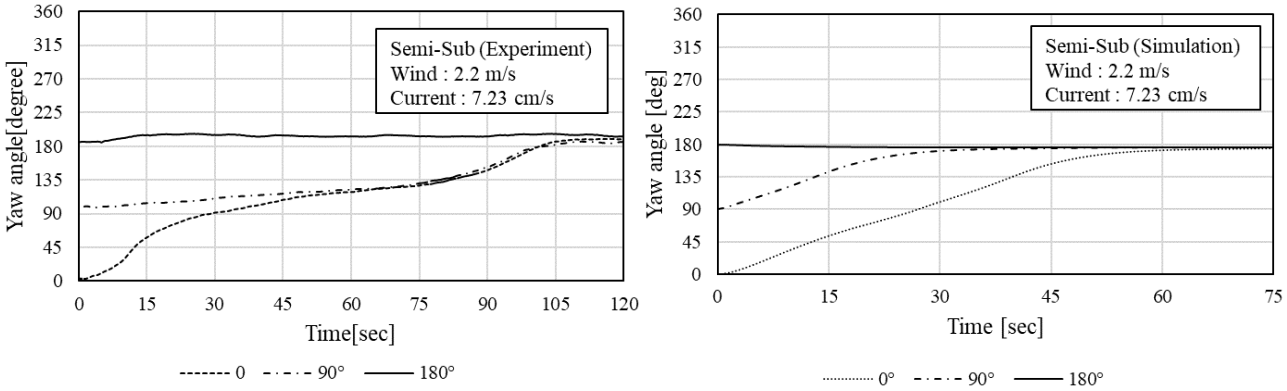

(a) Experimental result (b) Simulation result

Figure 17: Semi-Sub model in wind-current coexisting condition (V_{w0} = 2.2 m/s, V_{c0} = 7.23 cm/s)

Similar observations are made for the case of current speed of 7.23 cm/s. The Semi-Submersible type takes so long time to follow the wind direction in the experiment (around 1 min 42 sec for initial angle of 0

degrees). This response corresponds to about 23 minutes in the real scale. Table 6 shows the response time of the Spar and Semi-Submersible type at each current speed. The response time indicates time from initial angle of 0 degrees to final angle of 180 degrees.

Table 6: Response time for initial angle of 0 degrees

Types of floating body	**Current speed**	**Response time**	
		Model scale	Real scale
Spar	3.69 cm/s	6.6 sec	1 min 33 sec
	7.23 cm/s	14.8 sec	3 mins 29 sec
Semi-Submersible	3.69 cm/s	36.7 sec	8 mins 39 sec
	7.23 cm/s	1 min 41.5 sec	23 mins 55 sec

Figures 18 and 19 show the (a) experimental and (b) simulation results of spar type and Semi-Sub type in the severe current condition (V_{w0} = 2.2 cm/s, V_{c0} = 11.0 cm/s). Because of the severe current force, Semi-Sub type is not able to follow the wind direction for any initial angle in both experiment and simulation (see Figure 19). It balances at around 45 degrees instead of the expected 180 degrees. In this case, Semi-Sub type can't generate electricity power efficiency because the misalignment is too large. From the view point of safety, it will be necessary to shut down the wind turbine and stop the rotor during extreme conditions of current.

The unstable oscillations of spar type can be observed around 180 degrees in the experiment. This oscillation induces extra load to the blades and tower of the wind turbine, and may lead to failure of the model structurally. On the other hand, the oscillation of spar type cannot be observed in the simulations. In the future study, it is necessary to further improve the simulation method to evaluate the oscillation in the simulation.

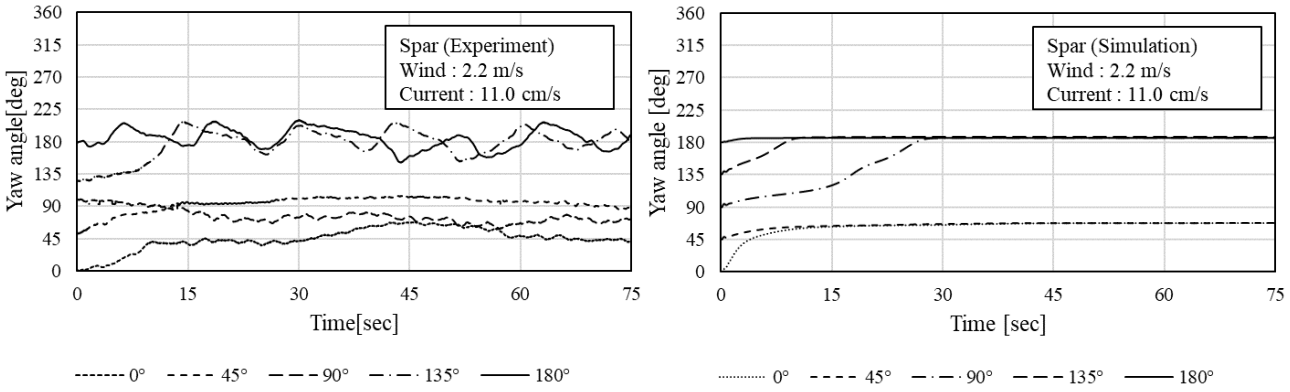

(a) Experimental result (b) Simulation result

Figure 18: Spar model in the severe current condition (V_{w0} = 2.2 cm/s, V_{c0} = 11.0 cm/s)

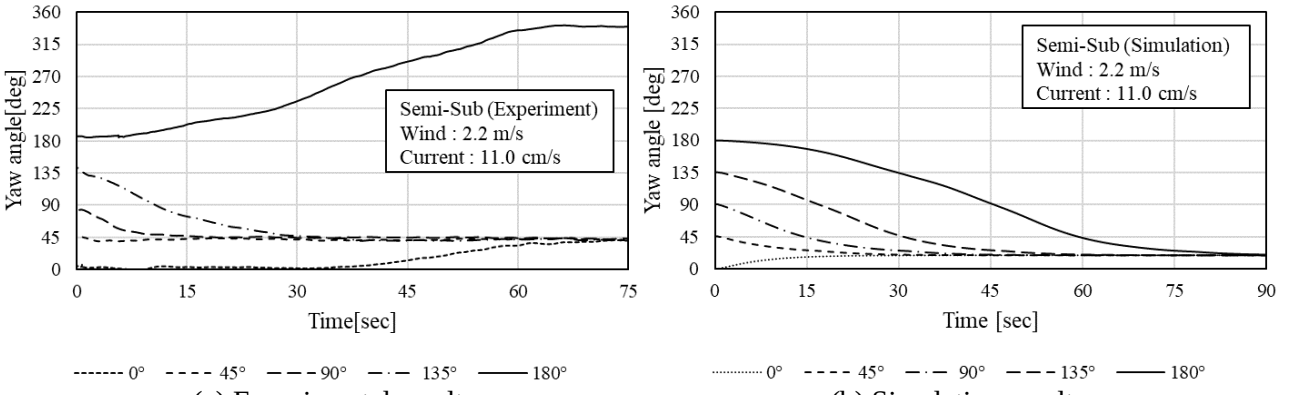

(a) Experimental result (b) Simulation result

Figure 19: Semi-Sub model in severe current condition (V_{w0} = 2.2 cm/s, V_{c0} = 11.0 cm/s)

6 CONCLUSION

In this study, weathervane performance and stability of two types of FOWTs moored to SPM system in the wind-current coexisting field are verified and compared by scaled model experiments and numerical simulation. The experiment is conducted using1/200 scaled models of spar and Semi-Sub type, based on Froude's scaling law. And the numerical simulation program is developed assuming the SPM-FOWTs modelled as two rigid bodies. Following specific conclusions can be derived.

- It is found from experiment and simulation that both of the spar and Semi-Submersible type can follow the wind direction in the slow current conditions. The response time which can be defined as the time taken for the FOWT to attain the final position from the initial position, varies according to the type of the floating body and current speed.

- The response time of Semi-Submersible type tends to be longer than that of spar type. This is because, Semi-Sub type is affected by the current load and moment more than spar type. It is also found that the response time becomes longer, as the current speed increases when the wind speed is constant.

- It is found from the result of the simulation, the FOWTs of the simulation follows the wind direction faster than the experiments. This discrepancy between simulation and experiments can be because the damping force due to water is not considered in the simulation. It is necessary to evaluate the force due to water more accurately in the future.

- The oscillation of spar is observed during the severe current condition. This oscillation induces extra load to the blades and tower of the wind turbine, and may lead to failure of the model structurally. However, the oscillation of spar type cannot be observed in the simulation. In the future study, it is necessary to improve the simulation method to simulate the unstable oscillation, and find the cause and solution of oscillation.

REFERENCES

[1] T. Ishihara. "Fukushima Floating Wind Farm Demonstration Project(1) – The Challenge towards the World's First Floating Wind Farm". In: *journal of the JIME,* Vol. 50, No. 1 (2015), 14-19

[2] Peter T. "How monitoring improves reliability & availability of offshore wind turbines & lower Cost of Energy". In: *A Creation donation course of the next-generation wind power generation system*, Vol. 2 (2014), 9-38.

[3] Nihei Y., Matsuda Y., Kitamura S., Takaiwa K. and Kanda N. "Research and development about the mechanisms of a single point mooring system for offshore wind turbines". In: *Ocean Engineering*, Vol. 147 (2018), 23.-31.

[4] Murai M., Nihei Y., Matsura M. and Takahashi K., "An experimental study on wind-following response of single-point mooring type offshore wind turbine", In: *JASNAOE Spring Meeting*, (2014).

[5] 3) J.Jonkman, S.Butterfield, W.Musial, and G.Scott. "Definition of a n 5-MW Reference Wind Turbine for Offshore System Development". In: *Technical Report NREL*, TP-500-38060(2009)

[6] Iijima K., Kuroda Y., Nihei Y. and Murai M. "Comparison of Weathervane Performance Between Two Types of FOWT Systems Moored to SPM". In: *ASEM 2015 34th International Conference on Ocean, Offshore and Arctic Engineering*, Vol. 8